the plant journal

SEB Society for Experimental Biology

The Plant Journal (2018) doi: 10.1111/tpj.13918

TECHNICAL ADVANCE

Photoinducible DRONPA-s: a new tool for investigating cell–cell connectivity

Nadja Gerlitz[1], Richard Gerum[2], Norbert Sauer[1] and Ruth Stadler[1,*]

[1]*Molecular Plant Physiology, University of Erlangen, Staudtstrasse 5, Erlangen 91058, Germany, and*
[2]*Biophysics, University of Erlangen, Henkestrasse 91, Erlangen 91052, Germany*

Received 22 December 2017; revised 2 March 2018; accepted 26 March 2018.
*For correspondence (e-mail ruth.stadler@fau.de).

SUMMARY

The development of multicellular plants relies on the ability of their cells to exchange solutes, proteins and signalling compounds through plasmodesmata, symplasmic pores in the plant cell wall. The aperture of plasmodesmata is regulated in response to developmental cues or external factors such as pathogen attack. This regulation enables tight control of symplasmic cell-to-cell transport. Here we report on an elegant non-invasive method to quantify the passive movement of protein between selected cells even in deeper tissue layers. The system is based on the fluorescent protein DRONPA-s, which can be switched on and off repeatedly by illumination with different light qualities. Using transgenic *35S::DRONPA-s Arabidopsis thaliana* and a confocal microscope it was possible to activate DRONPA-s fluorescence in selected cells of the root meristem. This enabled us to compare movement of DRONPA-s from the activated cells into the respective neighbouring cells. Our analyses showed that pericycle cells display the highest efflux capacity with a good lateral connectivity. In contrast, root cap cells showed the lowest efflux of DRONPA-s. Plasmodesmata of quiescent centre cells mediated a stronger efflux into columella cells than into stele initials. To simplify measurements of fluorescence intensity in a complex tissue we developed software that allows simultaneous analyses of fluorescence intensities of several neighbouring cells. Our DRONPA-s system generates reproducible data and is a valuable tool for studying symplasmic connectivity.

Keywords: plasmodesmata, cell–cell communication, photoactivation, DRONPA, *Arabidopsis thaliana*, root tip, technical advance.

Linked article: This paper is the subject of a Research Highlight article. To view this Research Highlight article visit https://doi.org/10.1111/tpj.13946.

INTRODUCTION

The exchange of molecules between cells is essential for the development of multicellular organisms. Plants have evolved a unique intercellular communication system based on plasmodesmata, which form a supracellular symplasmic network and allow molecules to move between cells (Lucas and Lee, 2004).

The 'default' state in plant tissues is thought to be open plasmodesmata (Brunkard and Zambryski, 2017). Only a few specialized cells such as sperm cells and guard cells become isolated during differentiation (Willmer and Sexton, 1979; Wille and Lucas, 1984; Palevitz and Hepler, 1985). However, the size exclusion limit (SEL), which is defined as the molecular weight of the largest molecules (in kDa) that can diffuse cell-to-cell, is specific to the type of cell. Generally, the aperture of plasmodesmata can be reduced by callose deposition at their neck region, thereby expanding the cell wall and mechanically narrowing the pore. This process can be reversed by the activity of a callose-degrading β-1,3-glucanase, which causes reopening of plasmodesmata (see Amsbury *et al.*, 2018, for a recent review).

Cell-to-cell movement of proteins and regulatory RNAs is essential for establishing cellular identity in meristematic tissues (Otero *et al.*, 2016). Transgenic Arabidopsis lines with blocked plasmodesmata in the globular embryo or in the endodermis of the root meristem developed severe defects in tissue patterning (Vatén *et al.*, 2011; Lu *et al.*, 2018). Generally, cells of undifferentiated tissues contain

large and unbranched plasmodesmata that allow the exchange of signalling molecules involved in cell differentiation processes (Zhu *et al.*, 1998a,b; Oparka *et al.*, 1999; Burch-Smith and Zambryski, 2010). During development, plasmodesmata can be modified to branched structures, often accompanied by a reduction in their SEL (Oparka *et al.*, 1999; Burch-Smith and Zambryski, 2010; Fitzgibbon *et al.*, 2013). The regulation of the aperture of plasmodesmata is important for a number of physiological processes, for example the coordinated response to stress conditions. Abiotic stress, such as exposure to cadmium or aluminium, as well as cold or wounding lead, to callose deposition within minutes (Sivaguru *et al.*, 2000; Ueki and Citovsky, 2005; Jones *et al.*, 2006; Bilska and Sowinski, 2010). Pathogen infection also leads to a closure of plasmodesmata. The chitin receptor LYSIN MOTIF DOMAIN-CONTAINING GLYCOSYLPHOSPHATIDYL-INOSITOL-ANCHORED PROTEIN 2 (LYM2) and the flagellin receptor FLAGELLIN-SENSING 2 (FLS2) mediate the response to fungal and bacterial pathogens, respectively (Gómez-Gómez and Boller, 2000; Faulkner *et al.*, 2013; Cheval and Faulkner, 2018). PLASMODESMATA LOCATED PROTEIN 5 (PDLP5), a receptor-like protein that is activated by salicylic acid (SA), is involved in the signalling pathway that leads to the accumulation of callose at the neck region of plasmodesmata during plant immune responses (Thomas *et al.*, 2008; Lee *et al.*, 2011; Cui and Lee, 2016; Lim *et al.*, 2016). Several independent studies indicate a link between callose deposition and reactive oxygen species (ROS) such as hydrogen peroxide and superoxide (Benitez-Alfonso *et al.*, 2010; Oide *et al.*, 2013). The regulation of plasmodesmal aperture is not only important to restrict or allow movement of proteins or RNA during development or upon stress treatment; it rather is likely that the intercellular movement of all kinds of molecules is controlled according to their size or nature. Several facts point towards SEL regulation having a part in establishing or maintaining auxin gradients (Jackson, 2015). The tight regulation of the aperture is also thought to play a role in discriminating between different sugars. According to the polymer trap model, plasmodesmata of plant species that transport raffinose in the phloem can discriminate between di- and trisaccharides (Turgeon and Gowan, 1990; McCaskill and Turgeon, 2007; Liesche and Schulz, 2013).

It is well established that plasmodesmata are highly dynamic and flexible structures and that the tight regulation of their structure and SEL is central for the control and regulation of symplasmic connectivity (Schulz, 1999; Roberts and Oparka, 2003). Several attempts have been made to study the degree of symplasmic coupling of plant cells. Much information on the structural organization of plasmodesmata has been obtained through transmission electron microscopy (Robards, 1971; Gunning, 1978; Ding *et al.*, 1992; Botha *et al.*, 1993; Overall and Blackman, 1996; Waigmann *et al.*, 1997). For some tissues the ultrastructure or frequency of plasmodesmata have been well characterized (Zhu *et al.*, 1998a,b; Fitzgibbon *et al.*, 2010; Bell and Oparka, 2011; Ross-Elliott *et al.*, 2017). However, it is impossible to predict the aperture of plasmodesmata based on structural analyses and, whereas the absence of plasmodesmata is clear evidence for a lack of symplasmic connectivity, their presence in a cell wall does not necessarily mean that they are functional. Therefore other techniques have been developed to demonstrate their functionality.

Intercellular resistance has been measured using electrophysiological approaches based on the fact that electric signals spread through open plasmodesmata (Holdaway-Clarke *et al.*, 1996, 2000). Other studies focused on analyses of symplasmic cell-to-cell movement of small fluorescent dyes like fluorescein isothiocyanate and carboxyfluorescein or of larger fluorescent dextrans (Tucker, 1982; Wolf *et al.*, 1989; Oparka *et al.*, 1995; Rinne and van der Schoot, 1998; Fisher and Cash-Clark, 2000). Permeable dyes like carboxyfluorescein diacetate (CFDA), which are processed inside the cells and converted into membrane-impermeable fluorescent dyes, were used to investigate phloem unloading and symplasmic connectivity in sink tissues (Wright and Oparka, 1996; Roberts *et al.*, 1997; Haupt *et al.*, 2001; Stadler *et al.*, 2005a). The drop-and-see (DANS) assay was developed to investigate the symplasmic spread of carboxyfluorescein through a leaf. After dropping CFDA on the adaxial epidermal surface of an intact leaf, tracer appearance was monitored in the abaxial epidermis (Lee *et al.*, 2011). Photoactivation experiments with caged fluorescein were performed to quantify cellular coupling in leaves (Martens *et al.*, 2004; Liesche and Schulz, 2012, 2013). Fluorescence recovery after photobleaching (FRAP) was used to study plasmodesmal permeability and continuity of the endoplasmic reticulum (ER) between cells (Grabski *et al.*, 1993; Martens *et al.*, 2006). Rutschow *et al.* (2011) investigated the cell-to-cell movement of a carboxyfluorescein derivative in roots of *Arabidopsis thaliana*, combining FRAP with a mathematical model.

One disadvantage of the use of small dyes for monitoring symplasmic coupling is that it doesn't provide any information on the possible passive movement of proteins as these dyes can also pass plasmodesmata with very small SEL. To analyse passive protein movement, cDNAs coding for fluorescent proteins were bombarded into epidermal cells and cell-to-cell spread was monitored (Oparka *et al.*, 1999; Crawford and Zambryski, 2000; Faulkner *et al.*, 2013). However, a major drawback of bombardment- or microinjection-based methods is that they are invasive and can trigger wound-induced changes in SEL. To avoid wounding effects, cDNAs coding for fluorescent proteins were expressed in single cell types or tissues and cell-to-cell spread was monitored (Imlau *et al.*, 1999; Stadler

et al., 2005a,b; Rim *et al.*, 2009) However, for each cell type analysed a new transgenic line had to be generated. Furthermore, despite the use of inducible promoters these analyses had a low temporal resolution in the range of hours or days (Roslan *et al.*, 2001). Photoactivatable GFP (paGFP) was used to monitor passive protein movement between cells in *35S*promoter:pa*GFP* lines; however, these analyses were restricted to cells at the tissue surface such as leaf or root epidermis cells or cells of isolated two-celled embryos (Li *et al.*, 2013; Nicolas *et al.*, 2017). Similarly, the utility of the photoswitchable fluorescent proteins Dendra and EosFP was limited due to a low efficiency of photoconversion in deeper layers (Wu *et al.*, 2011).

Although there are a several techniques available today, it is still not possible to analyse passive protein movement with high temporal resolution in cells that are not at the tissue surface. However, information on passive protein movement is crucial for the understanding of developmental processes, especially in deeper layers of root and shoot meristems. The present paper describes analyses of cellular connectivity in the root meristem using a new non-invasive method allowing comparative analyses of symplasmic connectivity of single cells with high spatial and temporal resolution in deeper tissue layers. Using a single transgenic Arabidopsis line it was possible to analyse any cell type in the root meristem with regard to its symplasmic connectivity to neighbouring cells. The system is based on the coral-derived 28-kDa DRONPA-s protein that can be repeatedly photoconverted from a fluorescent 'on' state into a non-fluorescent 'off' state and vice versa (Ando *et al.*, 2004; Lummer *et al.*, 2011). Using a confocal microscope equipped with a two-photon laser, it was possible to activate DRONPA-s in inner layers of the root tip yielding a bright green fluorescence in single cells. Fluorescence intensities were quantified 10 min after activation to monitor passive protein movement out of the activated cell into neighbouring cells. The data demonstrated cell-type-specific differences in total protein efflux capacities as well as differences in the symplasmic connectivity of one specific activated cell to different adjacent cells.

RESULTS

Setting-up the DRONPA-s system

We generated transgenic Arabidopsis plants expressing *DRONPA-s* under control of the *35S* promoter (*35S:: DRONPA-s*). In these plants, the steady-state condition of DRONPA-s is the fluorescent state (Figure 1a). In order to deactivate the fluorescence, root tissue was exposed to high-intensity 488-nm laser light. After deactivation, the DRONPA-s signal was no longer detectable throughout any of the layers of the root tip (Figure 1b–d). Exposure of a region of interest (ROI) in a single cell with 800-nm light produced by a two-photon-laser restored DRONPA-s fluorescence (Figure 1c, d, asterisk). Although only a small area was irradiated, fluorescence was recovered in the entire cell (Figure 1e, f, asterisk) due to diffusion and cytoplasmic streaming within the cell. The two-photon setup was used for fluorescence reactivation in all experiments to avoid activation in layers below and above the focal plane. Optical longitudinal and cross sections of the root confirmed the assumption that the use of a two-photon laser enabled activation of single cells exclusively in the focal plane (Figure 1d–f) without damaging the cells due to the low energy content of the photons. Single-cell excitation was controlled optically by taking a picture immediately after activation (t = 0 min) (Figure 1e). DRONPA-s fluorescence was occasionally activated in two neighbouring cells when the ROI was placed too close to the plasma membrane of the neighbouring cell. However, most of the time only the activated cells showed strong green fluorescence immediately after activation, while neighbouring cells showed either no or only weak fluorescence. This weak fluorescence was independent of the distance of the ROI to the neighbouring cell and very likely due to DRONPA-s flux occurring during the activation period. Movement of DRONPA-s to the adjacent cells was monitored 10 min after single-cell activation (t = 10 min; Figure 1g, j).

For quantification, fluorescence intensity was measured using the Leica Software LAS AF. Circular ROIs were placed in the centre of the activated and neighbouring cells in t = 10 min images (Figure 1g, j). Within the individual ROIs the brightness of green pixels was measured and the intensity per area was determined. Then the area of each cell was measured manually and multiplied by the corresponding intensity per area. The resulting fluorescence value across the entire individual cell is hereinafter referred to as 'total fluorescence', assuming that the fluorescence value in the focal plane is representative of the total number of DRONPA-s molecules in the entire three-dimensional cell. The sum of the total fluorescence of all cells in a measurement, the activated and the directly adjacent cells, was set as 100 fluorescence units (FU). Subsequently, the total fluorescence of the individual cells was normalized to this value. Flux quantification was established by comparing the FU in the activated cell and in all adjacent cells, as shown in Figure 1(k). The first bar reveals the total fluorescence of the activated epidermal cell (Ep) 10 min after photoactivation of DRONPA-s as an average value for 20 activated cells. The following bars represent the values for directly adjacent cells. The diagram shows that almost 50% of the FU were detectable in the activated cell. The longitudinal diffusion of DRONPA-s in the epidermis led to the detection of approximately 20 FU in each of the adjacent epidermal cells. Less than one-tenth of total fluorescence was detectable in adjacent cortical cells (lateral movement). The weakest fluorescence was detectable in

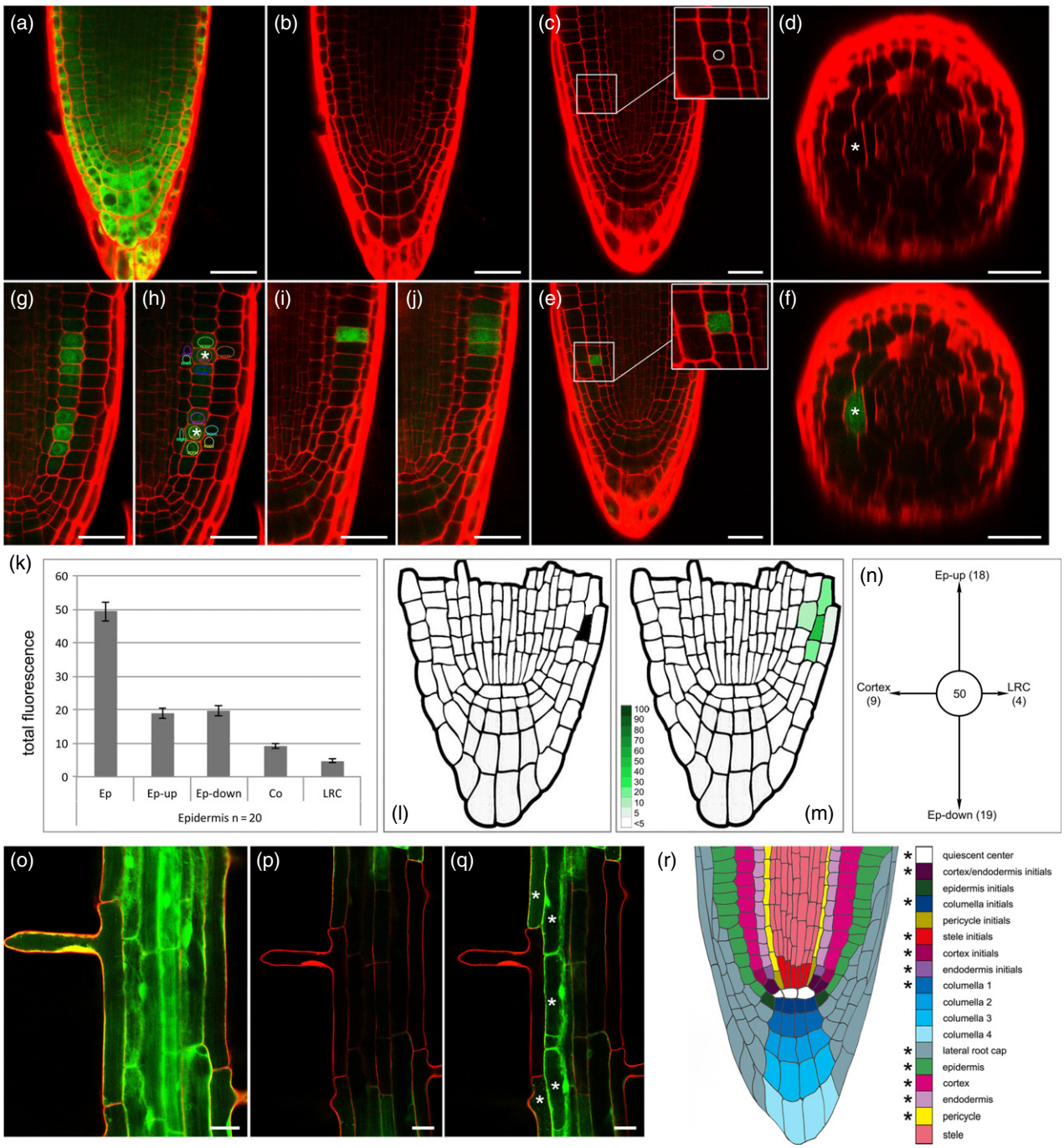

Figure 1. Setting-up the DRONPA-s system.
(a)–(j), (p)–(r) Roots of 3-day-old *35S::DRONPA-s* seedlings. (a) Untreated root tip with active DRONPA-s. (b) The same root as in (a) after deactivation of DRONPA-s. (c)–(f) Root tip before (c, d) and immediately after (e, f) reactivation of DRONPA-s in a cortex cell shown in higher magnification in the inlays in (c) and (e). The white circle in (c) represents the region of interest (ROI) for DRONPA-s reactivation. (d), (f) Optical cross section (*xz*-scan). (g), (h) Root tip 10 min after DRONPA-s activation in two cortex cells; the coloured circles in (h) represent the ROIs selected for fluorescence quantification. (i), (j) Root tip with activated epidermal cell 0 min (i) and 10 min (j) after activation. (k)–(n) Quantification of DRONPA-s flow shown in (j). (k) Bar diagram representing the normalized fluorescence intensities calculated as fluorescence units (FU): Ep, epidermis; LRC, lateral root cap; Ep-up, epidermal cell above the activated cell; Ep-down, epidermal cell below the activated cell. (l), (m) Coloured scheme: in (l) the activated cell is shown in black and in (m) the green colour gradient represent FU. (n) Circle diagram: circle, activated cell; arrows, flow direction and fluorescence intensity (length relative to FU); numbers represent FU. (o)–(q) Root differentiation zone before (o) and after (p) DRONPA-s deactivation and 10 min after (q) reactivation of DRONPA-s in selected cortex and epidermal cells. (r) Cartoon of a root tip: asterisks mark analysed cell types. In (a)–(q): green, DRONPA-s; red, propidium iodide stained cell walls; asterisks mark the cell selected for DRONPA-s activation. Scale bar = 25 μm.

the cells of the lateral root cap (LRC, below 5 FU). In the root tip scheme (Figure 1l, m), the colour gradations represent different total fluorescence values of individual cells in FU. In addition, the results of the measurement were visualized in a circular diagram indicating the orientation in the tissue (Figure 1n).

Generally, the data generated by the DRONPA-s system were highly reproducible, as indicated by the small error bars in the diagram in Figure 1(k). In addition, a single root could be repeatedly deactivated and activated without a detectable change in protein efflux capacity. This suggests that the treatment does not cause cell damage, which leads to the closure of plasmodesmata. Altogether the results indicate that DRONPA-s is well suited for measuring passive protein efflux.

DRONPA-s efflux in different root cell types

First we investigated cells in the root differentiation zone of a 3-day-old seedling. DRONPA-s was deactivated quantitatively in a root over a length of about 300 μm (Figure 1o, p). Fluorescence was then photoactivated in all cells except individual root hair cells in four independent experiments. Subsequent microscopic analyses showed that no DRONPA-s fluorescence was detectable in root hair cells even 20 min after photoactivation (Figure 1q). Similarly, there was no efflux of DRONPA-s into the neighbouring cells detectable 10 min after activation of a single root hair cell or a single differentiated epidermal cell (Fig. S2 in the online Supporting Information). This indicates that the plasmodesmal aperture of root hair cells in the differentiation zone is less than 28 kDa. In the phloem, DRONPA-s fluorescence was visible shortly after deactivation, indicating a high symplasmic connectivity of sieve elements (Figure S2b, d). However, fluorescence intensity measurements and quantification analyses in these cells were very difficult due to the large vacuoles of differentiated cells, which restrict the cytosolic cell content to the region close to a cell wall.

Twelve cell types were selected for analyses of cell–cell connectivities in the meristematic zone of the root (Figure 1r, asterisks). The fluorescence intensities were measured 10 min after fluorescence activation as described above. Examples of confocal images that had been used for quantification are shown in Figure 2. Average values were calculated from 10 to 30 independent measurements of each cell type (Figure 3). Where two cells were located adjacent to a single cell wall of the activated cell, both cells were measured as a single unit.

The first bar of each flux diagram shown in Figure 3 represents the normalized fluorescence, which was retained in the activated cell after 10 min. A high first bar indicates a low efflux capacity of the respective activated cell. The strongest movement of DRONPA-s was observed between pericycle cells and adjacent cells (Figures 2a, b and 3a). Only about 25 of 100 FU were retained in the pericycle cell, 75 FU were detected in the adjacent cells. This indicates that the large majority of DRONPA-s molecules had moved out of the activated pericycle cell (Figures 2b and 3a).

Stele initials were also well connected, with about 30 FU in the activated cell, followed by endodermis cells (33 FU), cortex cells (37 FU) and quiescent centre (QC) cells (40 FU; Figures 2e, f and 3b). Among the QC neighbours, the strongest fluorescence (about 20 FU) was detectable in columella initials (flux downwards). The weakest fluorescence, about 10 FU, was observed in stele initials (flux upwards) and in cortex/endodermis initials (lateral flux).

The comparison of endodermis initials and meristematic endodermis cells (cells four to ten from the initial upwards) showed different DRONPA-s movement capacities. Significantly less DRONPA-s moved out of endodermis initials than out of meristematic endodermis cells (Figures 2i, j and 3). In addition, meristematic endodermis cells showed a stronger vertical flux, while endodermis initials showed stronger lateral flux. Analyses of cortex initials and meristematic cortex cells yielded similar results. A comparison of both cortex and endodermis cells with their respective initials showed that both initials were generally worse coupled than their daughter cells. Both initials allowed predominantly transverse flow, whereas meristematic cells showed a better longitudinal flow (Figures 2g, h and 3).

In cortex/endodermis initials, a uniform fluorescence distribution was detectable in all neighbouring cells (Figure 2c, d). Almost half of the activated DRONPA-s molecules diffused into the neighbouring cells.

Due to its position and orientation towards the QC, the columella initial cell layer was considered to be a domain. All columella initials were activated simultaneously (Figure S1). Ten minutes after activation, 50 FU were detected in the activated cells. The bulk of DRONPA-s (about 20 FU) diffused from the columella initials into the first columella layer C1 (downwards), slightly less (17 FU) moved upwards into the QC cells and 13 FU were detected in the epidermis initials (lateral flux). Analyses of C1 cells revealed a comparably weak total efflux with almost 60 FU in the activated C1 cells. Flow from C1 into columella initials (upwards) and into the second columella layer (downwards) was significantly higher than lateral flux to adjacent C1 cells.

The LRC had the lowest symplasmic connectivity in the root tip (Figures 2k, l and 3). More than 70 FU could be detected in activated LRC cells 10 min after activation. Fewer than 10 FU were measured in the neighbouring cells. This minimal fluorescence was not visible in the microscopic images (Figure 2k, l).

In summary, our analyses showed that all cells of the root meristem are symplasmically connected. However, the entire efflux differed between individual cells depending on the cell type and the stage of differentiation of the cell. Generally, the cells inside a tissue layer were better connected than the cells of different layers.

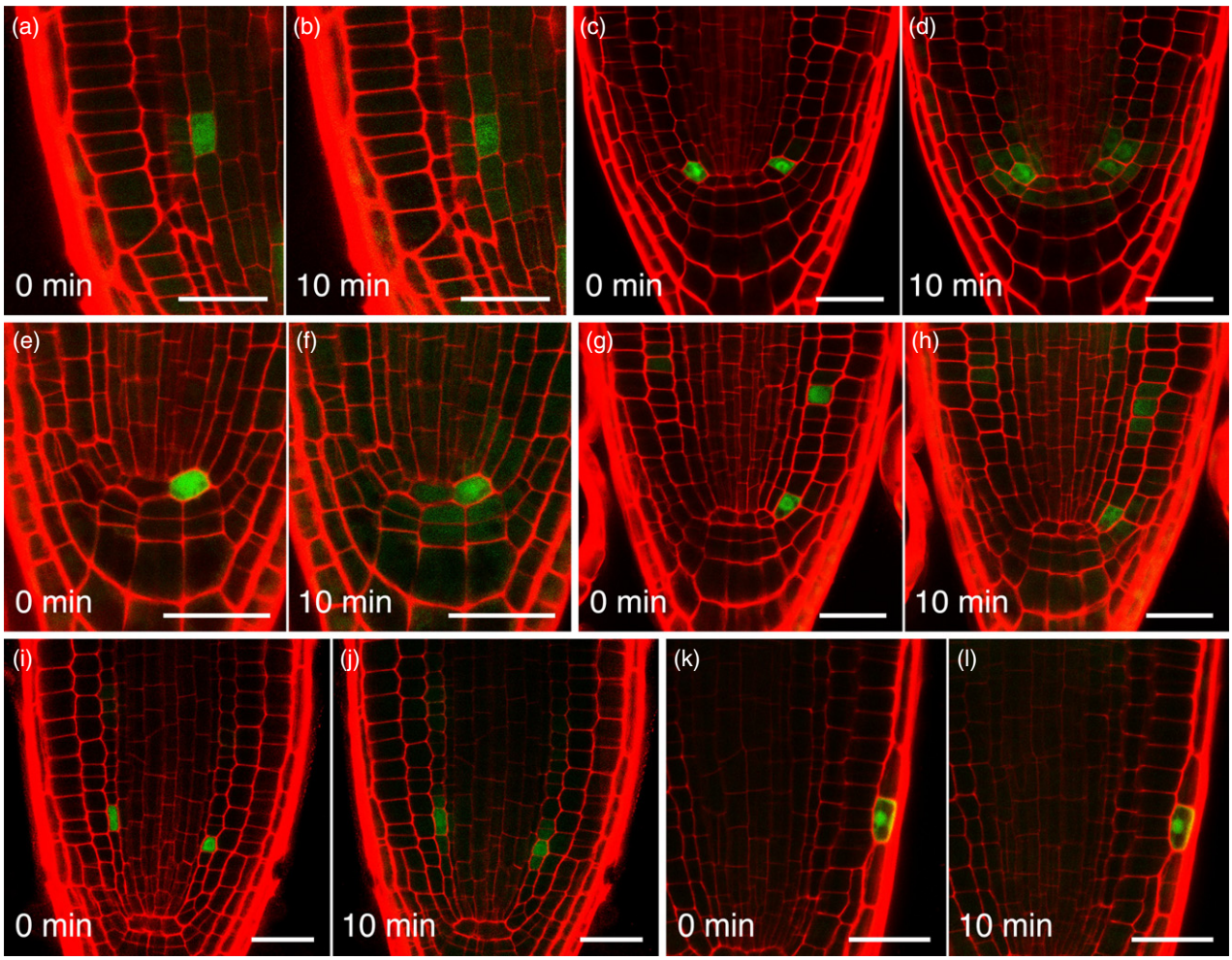

Figure 2. Cell-to-cell movement of DRONPA-s in root tips.
(a)–(l) root tips of 3-day-old *35S::DRONPA-s* seedlings: red, propidium iodide; green; DRONPA-s; time, min after DRONPA-s activation. (a), (b) Activated pericycle cell. (c), (d) Activated cortex/endodermis initial. (e), (f) Activated quiescent centre. (g), (h) Activated cortex initial and cortex cell. (i), (j) Activated endodermis cells. (k), (l) Activated lateral root cap. Scale bar: 25 μm.

Proof-of-concept: monitoring changes in plasmodesmal aperture

It has been published that stress treatments can lead to altered symplasmic connectivity. To prove the DRONPA-s system we analysed if it can be used to detect stress-induced changes in plasmodesmal aperture. For the biotic stress condition we chose the bacterial elicitor flagellin (flg22). Treatment with flagellin induced a weak but significant reduction of DRONPA-s efflux from activated cortex cells (Figure 4). We also tested SA, which is known to be involved in the response of the plant to bacterial pathogens by regulating cell–cell permeability in Arabidopsis leaves (Wang *et al.*, 2013). Roots of SA-treated seedlings showed a significant reduction in DRONPA-s efflux 10 min after DRONPA-s activation. In control plants, 35 FU were retained in activated cortex cells while in SA-treated roots 55 FU were retained, which reflects a reduction in the total efflux of about 30% due to SA treatment (Figure 4h). Chilling was selected as an abiotic stress condition. Cold-treated seedlings also showed a strong reduction of DRONPA-s efflux (Figure 4e–g). While cortex cells of control plants retained 35 FU, cells of cold-treated seedlings retained 73 FU. Taken together the data showed that stress-induced changes in plasmodesmal aperture can be monitored using the DRONPA-s system.

DRONPA-s flux in green tissues

To analyse the suitability of the system in other tissues we activated DRONPA-s in epidermal cells of leaves and in vascular cells of young developing seeds.

DRONPA-s was switched off in a large area of about 400 μm^2 of a cotyledon and a true leaf, and reactivated in selected cells (Figure 5a–f). For DRONPA-s reactivation a ROI had to be set, which covered an area containing cytoplasm. Mature epidermal cells contain a large central vacuole that occupies almost the entire volume of these cells

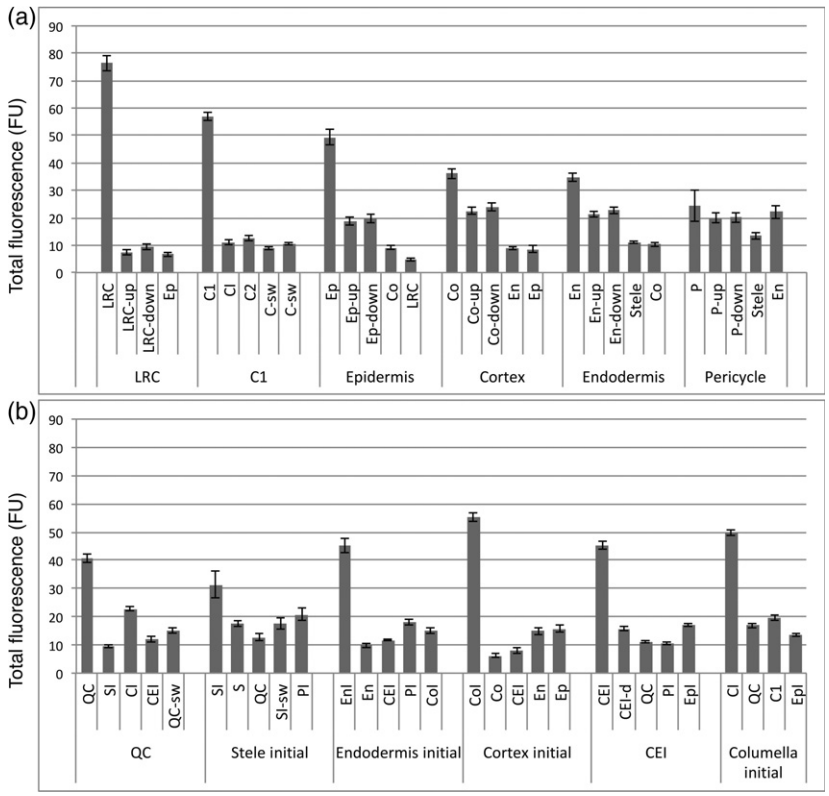

Figure 3. Graphical representation of DRONPA-s flow from 12 selected cell types.
(a), (b) Abscissa: investigated cell types. The first bar in each case is the activated cell and the following bars are direct neighbouring cells. QC, quiescent centre; SI, stele initial; CEI, cortex/endodermis initial; CSC, columella initial; EnI, endodermis initial; En, endodermis; PI, pericycle initial; CI, cortex initial; Ep, epidermis; CEI-t, cortex/endodermis initial daughter cell; EpI, epidermis initial; C1, first columella layer; C2, second columella layer; LRC, lateral root cap; P, pericycle; S, stele; -up and -down, cell above and below the activated cell; -sw, lateral adjacent cell.

and restricts the cytoplasm to a small layer lining the plasma membrane. One possibility was to place the ROI for DRONPA-s reactivation at the position of the nucleus, which is usually surrounded by cytoplasm. Another possibility was to set the ROI such that it covered the cell wall between two cells, which caused the activation of two cells instead of only one (Figure 5e, f). Often, the nuclei of some guard cells remained fluorescent after complete deactivation of the surrounding epidermal cells (Figure 5a, b, arrowheads). This fluorescence was still detectable even after prolonged deactivation phases and was not caused by influx of DRONPA-s from neighbouring cells, which were non-fluorescent. It is possible that the fluorescence was caused by new DRONPA-s synthesis because of high general transcriptional activity in guard cells or by insufficient deactivation. No flow of DRONPA-s from activated cells was detectable in the epidermis of either cotyledons or true leaves, even 20 min after activation (Figure 5b, c, e, f), suggesting that the SEL of the majority of plasmodesmata that connect epidermal cells in both leaf types is too small to allow rapid movement of DRONPA-s. Furthermore we tested whether developing Arabidopsis seeds can be examined for their symplasmic connectivity using the DRONPA-s system. Previous studies had shown that GFP synthesized in phloem companion cells was able to move from the funicular phloem into the so-called unloading domain of developing seeds (Stadler *et al.*, 2005a; Werner *et al.*, 2011). In this respect, it should be investigated if the flow of DRONPA-s can be analysed in the funiculus–ovule transition zone. For this purpose, developing seeds of flowers 1 day after pollination were stained with propidium iodide (PI). Complete deactivation of DRONPA-s in the whole tissue and a precise reactivation in selected cells could be achieved in these plant organs as well (see Figure 5g–j). DRONPA-s was activated in several cells in the area of the funiculus–phloem. Phloem cells are recognizable by their elongated and narrow shape and by their proximity to xylem cells with helically thickened cell walls. Fifteen minutes after activation, DRONPA-s fluorescence was visible in several cells of the unloading domain adjacent to the phloem (Figure 5i, j, arrows).

The results showed that DRONPA-s is well suited for the analysis of cell–cell connectivity, not only in roots but also in other plant organs. It could be successfully switched off and precisely switched on in selected cells of ovules and leaves.

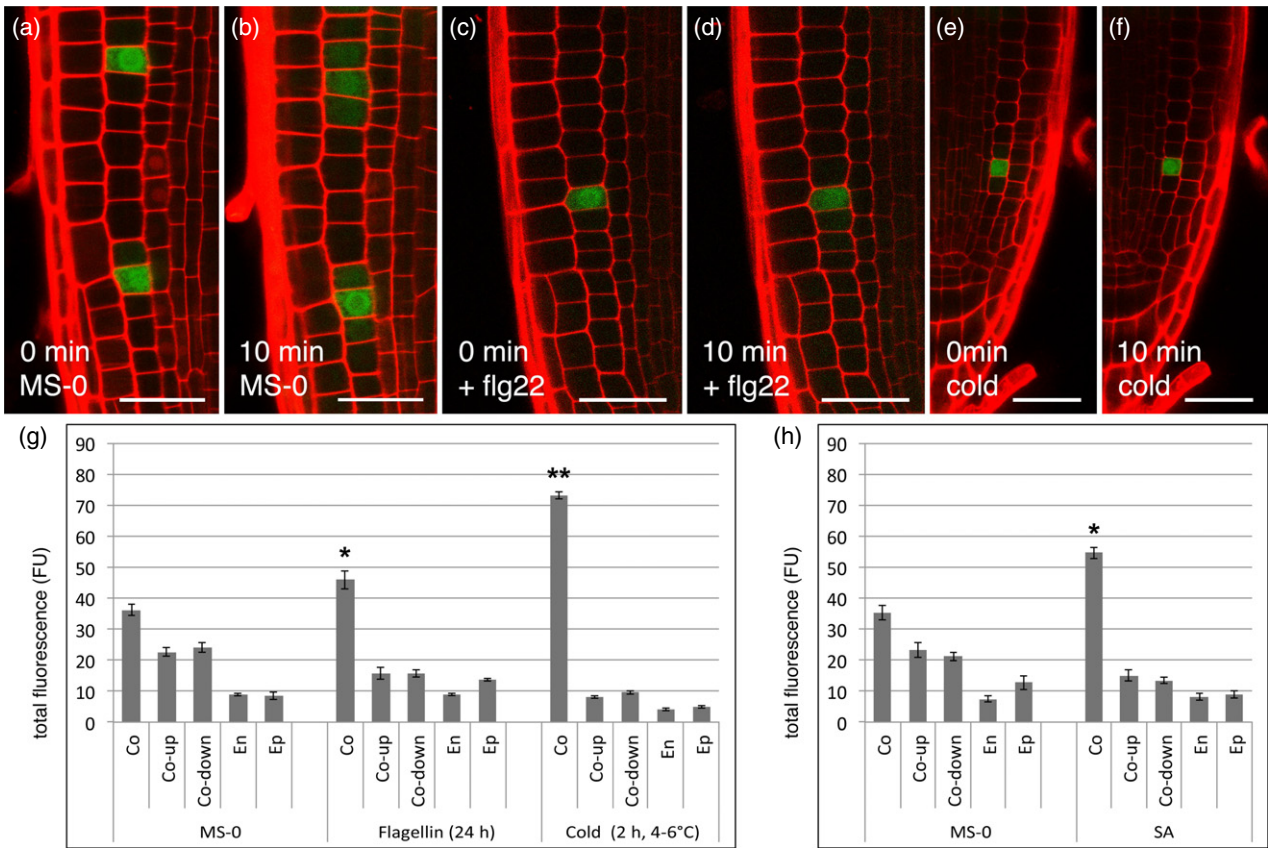

Figure 4. Cell-to-cell movement of DRONPA-s under stress conditions.
(a)–(f) Three-day-old roots: min, time after DRONPA-s activation in a single cortex cell; red, propidium iodide; green, DRONPA-s. (a), (b) Incubation on MS-0 under standard conditions. (c), (d) Two-hour incubation with flg22. (e), (f) Two-hour cold treatment. Scale bar = 25 μm. (g), (h) Quantification of DRONPA-s flow under different stress conditions. The abscissa shows investigated cell types. The first bar in each case is activated cortex cell and the following bars are neighbouring cells. Co, activated cortex cell; Co-up, cortex cell above the activated cell; Co-down, cortex cell below the activated cell; En, endodermis; Ep, epidermis; SA, salicylic acid.

Simulation of DRONPA-s flow and determination of diffusion constants

New software was developed in order to simplify the process of measuring fluorescence brightness. To quantify diffusion of DRONPA-s using this software, DRONPA-s was first activated in a cortex cell (Figure 6a) as described above. Ten minutes after activation of DRONPA-s total fluorescence was measured as the total pixel intensity summed over the cell region (Figure 6b). The sum of the total fluorescence of all cells in a measurement, namely the activated cell and the directly adjacent cells, was set to 100 FU. The total fluorescence of the individual cells was normalised to this value (Figure 6c, numbers in brackets). The results (light grey bars in Figure 6e) were comparable with those described in Figure 3(a) from 18 independent manual measurements of the DRONPA-s flow (dark grey bars Figure 6e) with respect to both the DRONPA-s flow dynamics as well as the total fluorescence values, indicating that the automated brightness measurement matched very well with the manually determined values. The automation of the evaluation of data generated with the DRONPA-s system offers a potential tool for large-scale experiments.

A further goal of this approach was to simulate the DRONPA-s flow. For this purpose it was first necessary to investigate whether the measured DRONPA-s flow could be described by a free diffusion dynamic. Therefore, six independent measurements were carried out, recording DRONPA-s distribution over time at 2-min intervals for 10 min after activation of DRONPA-s in a cortex cell (Figure 6f–i). In contrast to previous experiments, the signals in the green channel were only moderately enhanced during the recordings to avoid saturation effects at the time point 0 min after activation (Figure 6f). These images were used to determine the overall intensity changes by manually labelling the cell area (using ClickPoints; Gerum *et al.*, 2016; Data S1) and measuring the fluorescence intensity. The intensity in the activated cell showed an exponential decay in all six experiments (Figure 6j, black curve). This indicates free diffusion of DRONPA-s, in contrast to limited

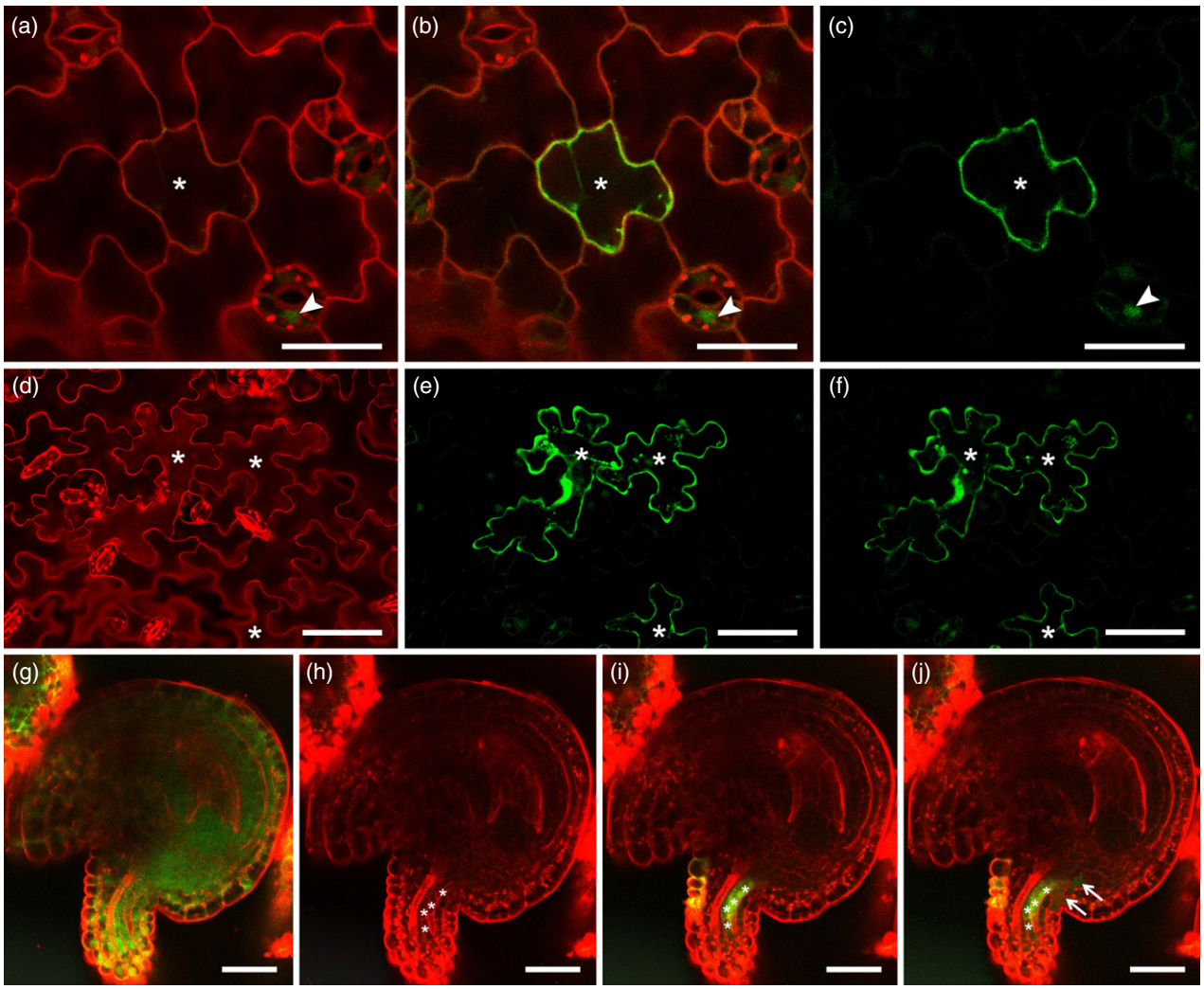

Figure 5. Cell-to-cell movement of DRONPA-s in other tissues.
(a)–(c) Cotyledon of a 3-day-old seedling prior (a), immediately after (b) and 20 min after (c) DRONPA-s activation in an epidermal cell. Arrowheads mark a fluorescent guard-cell nucleus. (d)–(f) True leaf of a 12-day-old seedling prior (d), immediately after (e) and 20 min after (f) DRONPA-s activation in two epidermal cells. (g), (h) Developing seed of a flower 1 day after pollination prior to (g) and after (h) DRONPA-s inactivation. (i), (j) Same seed as in (g) and (h) immediately (i) and 10 min after (j) DRONPA-s reactivation in a few phloem cells. Asterisks mark activated cells. Green, DRONPA-s; red, propidium iodide. Scale bar = 25 μm.

diffusion, which would result in linear decay. The fluorescence values in all adjacent cells initially increased. However, the values in the directly adjacent cortex cells above and below the activated cell decreased slightly after 4 min (Figure 6j, dark and light blue curves). This could be caused by general bleaching effects and by the loss of DRONPA-s into cells that are further from the activated cell and therefore not part of the measurement. A slightly increasing value was measured in the adjacent epidermal cells (Figure 6j, red and brown curves) and endodermis cells (Figure 6j, dark and light green curves).

Since the flow of DRONPA-s seems to follow a free diffusion, we tried to simulate the free diffusion to confirm this finding. The DRONPA-s intensity I in each cell was modelled to change in proportion to the concentration (intensity divided by the area) difference from the adjacent cells. For each cell wall between two given cells (c_i and c_j) a transport rate parameter was defined, here called the 'diffusion constant', D_{ij} (Figure 6k). To account for losses due to fluorescence bleaching and flow in cells outside the simulated region a loss parameter L was used, resulting in a rate equation for each cell:

$$\dot{I}_j - \sum_j D_{ij} \cdot (c_j - c_i) - L_i \cdot c_i$$

By fitting the parameters D_{ij} and L to the measured intensities, the DRONPA-s flow could be reproduced quite well. The simulated values (curves in Figure 6l) fit well to the measured values (dots in Figure 6l and curves in Figure 6j), representing the measurement shown in

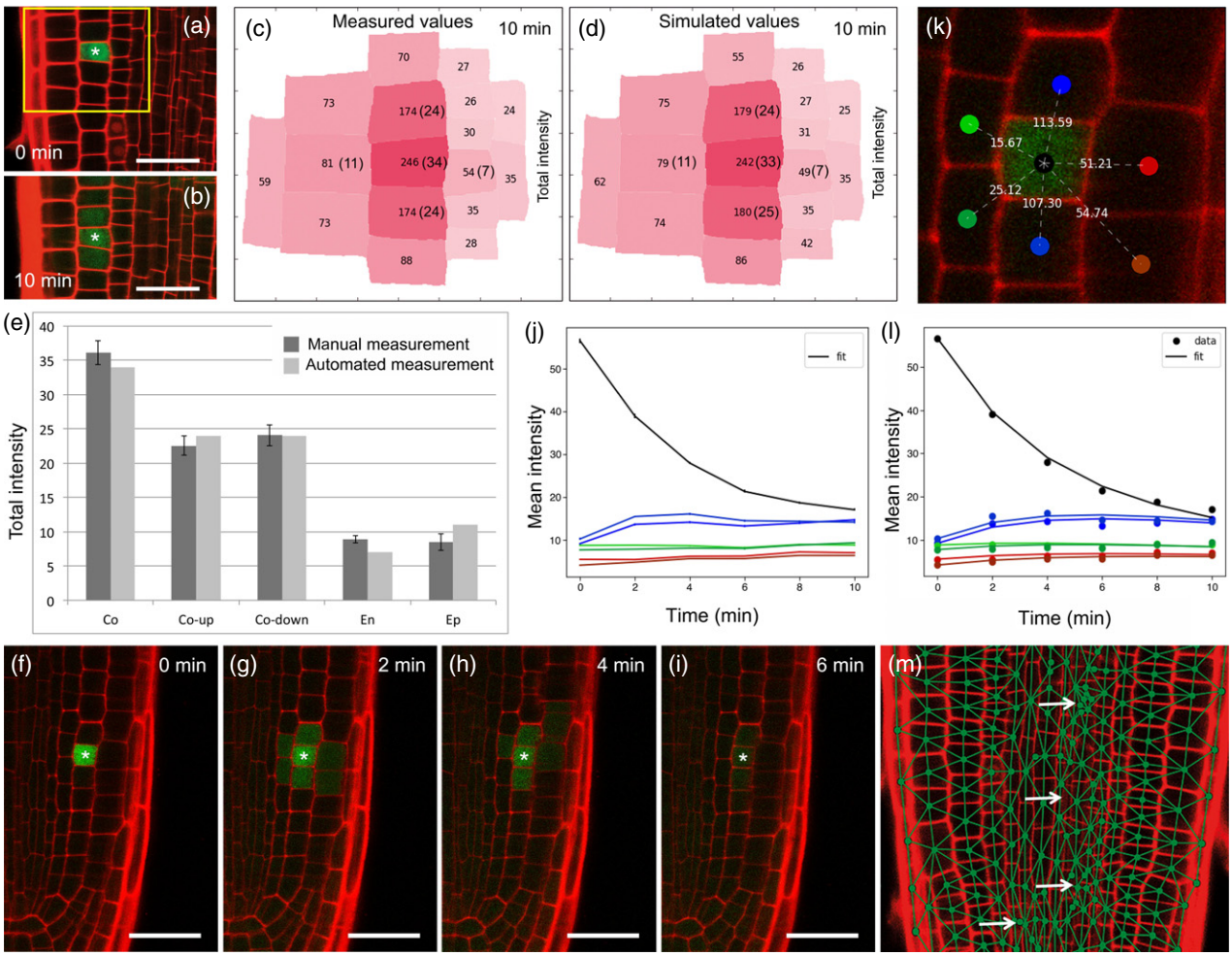

Figure 6. Automation and simulation of DRONPA-s flow out of a cortex cell.
(a), (b) Three-day-old root tip 0 min (a) and 10 min (b) after DRONPA-s activation. (c), (d) Schematic representation of measured values (c) and simulated values (d) of DRONPA-s intensities (indicated by the red hue) of the investigated cell group (yellow square in a): numerical values represent total intensity and numerical values in brackets represent normalised intensity. (e) Comparison of 18 manual (Figure 3) and one automatic (a–c) measurements of DRONPA-s flow. (f)–(i) DRONPA-s efflux at different time points after fluorescence activation as indicated. (j) Change of the average DRONPA-s intensity over time, measured in (f)–(i). Colour code applies to (j-l): activated cell (black); cortex cell below (dark blue) and above (light blue) the activated cell; adjacent endodermis cells (dark and light green); adjacent epidermal cells (red and brown). (k), (l) Modelled DRONPA-s flow corresponding to the measurement (f)(i) and fitted diffusion constants. (k) Determined diffusion constants. (l) Fit of the simulated (lines) to the measured (dots) values. (m) Root tip with automatically detected cell centres (green dots) and potential symplasmically connected neighbouring cells (green lines). Arrows mark areas which are difficult to recognize automatically. In (a), (b), (f)–(i), (k) and (m): asterisks, activated cells; green, DRONPA-s; red, propidium iodide. Scale bar = 25 μm.

Figure 6(f)–(i). The simulation also worked well with only two measurements at t = 0 min and t = 10 min (Figure 6d; representing the measurement shown in Figure 6a–c).

The model has some limitations as it only captures two-dimensional flow, ignoring flow in and out of the focal plane as well as flow in cells outside the simulated region. For details on the model, the fitting procedure and the limitations of the model see Data S2 'Flow model'.

The fact that the simulation values (Figure 6l) were nearly the same as the measured values and that they also correlated with the results from the previously described experiments suggests that these values represent the true symplasmic flow in the plant.

In order to automate the measurement process further software was developed for cell pattern recognition in PI-stained root tissue (Figure 6m). The automatic recognition of cell borders further facilitates automated measurement of fluorescence intensities in individual cells. However, in some areas of the root tip, such as the stele, the detection of single cells was difficult because of their small size and their irregular position (asterisks in Figure 6a, b). Therefore, the markings in these areas were controlled and, if necessary, corrected manually. This application could also be helpful for automating data analysis on a large scale, like the simultaneous analysis of different cell types in a complex tissue (for example the shoot meristem) or

temporal tracking of responses to stress conditions or mutant analyses.

DISCUSSION

We exploited the reversible photoactivation property of the fluorophore DRONPA-s to analyse symplasmic connectivity. The data showed that the symplasmic connectivity differs between the cell layers of the root tip.

Comparison of cell–cell connectivity in different cell types

The highest symplasmic connectivity was found between pericycle cells and their neighbours. In contrast to most other cell types, pericycle cells allowed strong lateral movement of DRONPA-s, primarily into the endodermis (Figure 3). This observation matches well with the pericycle's known function as a mediator for the exchange of signalling compounds between the stele and endodermis, which was shown to be essential for root development. SHORT-ROOT (SHR), for example, is synthesized in the stele and moves laterally via the pericycle into endodermis cells to determine their cell identity (Helariutta *et al.*, 2000; Nakajima *et al.*, 2001; Gallagher *et al.*, 2004; Sena *et al.*, 2004; Levesque *et al.*, 2006; Cui *et al.*, 2007, 2011). The regulatory microRNAs miR165/166 are synthesized in endodermis cells and move laterally into the stele. This gradient is also essential for root architecture (Carlsbecker *et al.*, 2010; Bishopp *et al.*, 2011; Miyashima *et al.*, 2011; Gallagher *et al.*, 2014).

Interestingly, endodermis and cortex initials had a better lateral connectivity than the meristematic cells derived from these initials. The fact that mother and daughter cells are differently well connected to neighbouring cells suggests different numbers of plasmodesmata or differently structured plasmodesmata in those cells. According to ultrastructural analyses, the number of plasmodesmata in longitudinal cell walls of the endodermis does not change with increasing distance to the QC (Zhu *et al.*, 1998a). Together with the DRONPA-s data, which demonstrate a decrease in lateral efflux from endodermis or cortex cells compared with their respective initials, this points towards a decreasing SEL of plasmodesmata in longitudinal cell walls. The analyses also indicate an increase in longitudinal flux inside of each layer and an increase of the SEL in the perpendicular cell walls with the age of the cell. It would therefore be interesting to specifically examine changes in symplasmic connectivity during cell maturation and root development.

A strong DRONPA-s efflux was also found in QC cells. In contrast to the other cells of the root meristem, QC cells don't divide very often, and their major task is to maintain the meristematic activity of the surrounding tissue. In this aspect the QC cells appear to be mature while the vast majority of the other cells in the root tip are meristematic. The fact that they appear to be even more strongly connected than columella initials or meristematic epidermis cells makes evident that meristematic activity is not a prerequisite for good symplasmic connectivity. It has been shown that several cell types reduce their cell–cell connectivity during maturation. This has been observed during embryo development (Rinne and van der Schoot, 1998; Gisel *et al.*, 1999) and during the transition from sink leaves to source leaves (Oparka *et al.*, 1999; Roberts *et al.*, 2001). Root epidermis cells have a high connectivity in the meristem and no connectivity in the differentiation zone, as shown for root hair cells (Duckett *et al.*, 1994; this work), and cells in tissue culture showed decreased symplasmic permeability during shooting (Cantrill *et al.*, 2001, 2005). However, studies on QC (this work) and on the sieve element–companion cell complex in source leaves that allows the passage of large molecules (Lucas *et al.*, 2001; Stadler *et al.*, 2005a,b), demonstrate that low connectivity is not a general feature of mature cells.

In contrast to most other cells in the root tip, the acropetal efflux capacity of QC cells (into columella initials) was more than twice the basipetal efflux (into stele initials). This observation fits well with the fact that the 26-kDa transcription factor WOX5, which is produced in the QC, also moves predominately down into columella initials to prevent cell differentiation (Pi *et al.*, 2015). However, it is also known that stele initials are well connected to the QC. SHR moves from the stele not only into the endodermis but also into the QC to ensure the maintenance of cell fate together with the transcription factors SCARECROW (SCR) and JACKDAW (JKD) (Welch *et al.*, 2007; Cui *et al.*, 2011; Ogasawara *et al.*, 2011). The acropetal efflux from columella initials and C1 cells (toward the root tip) was stronger than the basipetal flow. These data indicate that diffusion through plasmodesmata depends on the direction of the flow. Terry and Robards (1987) and later Christensen *et al.* (2009) found unidirectional symplasmic movement of fluorescent molecules in studies with trichomes of *Abutilon* and *Nicotiana*. Both the small fluorochrome Lucifer Yellow CH (LYCH) and photoactivatable GFP (paGFP) were able to move from the basal cell into the apical trichome cell, but not vice versa. Whether the directional flux of DRONPA-s is caused by mass flow or by specific funnel-like plasmodesmata, such as those connecting protophloem sieve elements with surrounding cells (Ross-Elliott *et al.*, 2017), remains to be elucidated. Three-dimensional analysis of plasmodesmata by means of super-resolution fluorescence live cell imaging (Fitzgibbon *et al.*, 2010) or electron tomography, as recently done by Nicolas *et al.* (2017), will provide further insights into this topic.

We observed a very low DRONPA-s efflux from LRC cells. One has to consider that LRC cells represent the tissue surface and therefore have fewer neighbouring cells than all other cell types. However, more than 75% of fluorescence

remained in LRC cells 10 min after activation compared with only 25-40% in highly connected cells. This indicates low connectivity of LRC cells. The outermost layer of the root cap including the LRC is fully differentiated. The cells are exposed to mechanical stress during growth through the soil and eventually undergo apoptosis, which could be a reason for the low symplasmic connectivity to neighbouring cells.

In summary we were able to show that the efficiency of passive protein movement between cells of the root meristem strongly differs depending on the cell type. Each cell of the root tip, especially around the QC, fulfils a unique programme due to positional effects. Therefore it is very likely that the need for cell–cell communication through plasmodesmata also varies between cell types. Generally, the observed differences in protein efflux capacity could be caused by a different number or aperture of plasmodesmata. For the root meristem, frequencies of plasmodesmata have been analysed by electron microscopy (Zhu *et al.*, 1998a,b). A comparison of both data sets showed that a high DRONPA-s efflux capacity correlates with a large number of plasmodesmata in the respective cell walls and a low efflux is reflected by a small number of plasmodesmata. In addition, the frequency of plasmodesmata in longitudinal walls of the endodermis is higher than in all other longitudinal cell walls, which fits with the high lateral efflux capacity from the pericycle into the endodermis. However, smaller differences in protein flux, like the two times stronger flux from QC into the columella than into the stele, are not reflected by the number of plasmodesmata, which is similarly high in both cell walls. This indicates that the structure and the aperture of plasmodesmata also influences cell-to-cell movement of proteins in the root meristem. For SEL analyses 2 × DRONPA-s or DRONPA-s fusion proteins of different sizes could be used. It has been shown that the switching between 'on' and 'off' states also works when DRONPA-s is fused to other proteins (Lummer *et al.*, 2011). In addition, latrunculin B could be used to analyse if cytoplasmic streaming also influences the capacity for passive protein movement between cells.

We also tested DRONPA-s activation in leaf epidermis cells and in developing seeds. After DRONPA-s activation in the funicular vasculature of ovules, fluorescence was visible in phloem unloading cells, as expected from previous data based on phloem mobile GFP (Stadler *et al.*, 2005a,b; Werner *et al.*, 2011). In contrast, no cell-to-cell movement of DRONPA-s could be detected in the epidermis of leaves, which at first glance seemed to contradict previous results. Several groups have shown that GFP can move through plasmodesmata between epidermal cells in mature leaves of *Nicotiana benthamiana* (Oparka *et al.*, 1999; Crawford and Zambryski, 2000; Liarzi and Epel, 2005) or Arabidopsis (Stonebloom *et al.*, 2012). However, in all those studies GFP movement was monitored at least 24 h after particle bombardment while in the present work DRONPA-s movement was analyzed 10–20 min after activation. Crawford and Zambryski (2000) observed that 23% of transformed leaf epidermis cells allowed diffusion of GFP 24 h post-bombardment and that the percentage of cells allowing diffusion increased on subsequent days. They hypothesized that the apertures of the plasmodesmata fluctuate, and initially undilated plasmodesmata could later adopt a dilated state. This indicates that it is very crucial to keep the observation time in mind when data on potential SELs are discussed. If cell-to-cell movement of DRONPA-s can be observed 10 min after photoactivation, this reflects that the majority of plasmodesmata have a SEL of at least 28 kDa, while no DRONPA-s movement would reflect that the majority of plasmodesmata have a SEL below 28 kDa. The latter seems to be the case for plasmodesmata between leaf epidermis cells and would also explain the slow movement of GFP after ballistic transformation of single epidermal cells which has been published by other groups. Considering this, the results of DRONPA-s analyses in leaf epidermis cells do not contradict previous results.

Changes of plasmodesmal aperture due to stress

As a proof-of-concept we tested if the DRONPA-s system can be used to detect stress-induced changes in cell–cell connectivity. Flagellin as well as SA treatment caused a reduction of DRONPA-s efflux from individual cortex cells of the root meristem. The bacterial peptide flagellin is one of the so-called microbe-associated molecular pattern (MAMP) molecules which are recognized by plant receptors and trigger various defence mechanisms. As an immune response to these elicitors, the molecular flux through plasmodesmata is reduced (Faulkner *et al.*, 2013; Sager and Lee, 2014; Stahl and Faulkner, 2016). Millet and co-workers (2010) observed callose accumulation in the mature zone and the elongation zone of roots after treatment with flagellin. We observed a weak but significant reduction of DRONPA-s flux in the meristem upon treatment with flagellin. This indicates that the DRONPA-s system is a very sensitive system for monitoring changes in SEL, probably more sensitive than callose staining with aniline blue. It has been hypothesized that SA is a mediator of the innate immune response to virulent bacterial infection as it is experimentally mimicked by treatment with flagellin (Wang *et al.*, 2013). This is consistent with our observation that SA treatments also caused a significant reduction in efflux of DRONPA-s from cortex cells. An even stronger decrease was visible upon cold treatment. That cold stress leads to closure of plasmodesmata was first observed in maize suspension cells using electrophysiological techniques. Chilling resulted in a fourfold increase in plasmodesmal resistance (Holdaway-

Clarke *et al.*, 2000). Bilska and Sowinski (2010) showed that cold treatment of leaves resulted in the accumulation of callose at the plasmodesmata of leaf mesophyll cells. The reduced efflux of DRONPA-s from root cells after cold treatment indicates that similar processes also occur in roots. Together, the data suggest that the DRONPA-s system is suitable for detecting stress-induced changes in plasmodesmal aperture.

Potentials and limitations of the DRONPA-s system

By using a mathematical software application we succeeded in automating cell boundary detection and the determination of fluorescence intensity. This automation increased the statistical significance of the results as well as the speed of data recovery and thus enables larger-scale-measurements. In addition, the DRONPA-s flow could be simulated and the values of the diffusion constants could be calculated for each individual cell boundary. The simulation enables a prediction of protein flow independent of time. Repeated flow simulations could be used to determine diffusion constants over cell walls for any cell of the root tip or other plant organs.

During our studies, some limitations of the DRONPA-s system became obvious. Activation of cells that are localized deep in the tissue was difficult. The cell walls need to be visualized, which could be problematic if the outer tissue layers limit dye perfusion. Transgenic plants with an RFP fusion protein anchored to the plasma membrane could be used to circumvent this problem. The cells should have a certain size, or if they are small at least a more or less regular pattern, otherwise it is hard to activate a single cell. If a cell contains a large vacuole it is easier to activate two cells and then the experimental setup has to be adjusted. Another drawback, however, is the fact that the DRONPA-s system is limited to plasmodesmata that allow 28-kDa DRONPA-s molecules to pass. Other methods have to be used to analyse plasmodesmata with a small SEL. However, the fact that DRONPA-s is not a small dye but a protein is also an advantage: it mimics the passive cell-to-cell movement of proteins, a process that is known to play a central role during plant development. Fusing DRONPA-s to plant proteins could permit their exact tracking, which up to now has only been possible via constitutive expression (Lummer *et al.*, 2011).

DRONPA-s is expressed under the control of the 35S promoter, which possibly has different activities depending on the cell type. However, the fact that there are not the same amounts of DRONPA-s molecules present in each cell does not interfere with the flux quantification. The amount of activated DRONPA-s represents only a small fraction of the molecules that are actually present in the target cell and also differs from experiment to experiment. However, the measured fluorescence is normalized to 100 FU to calculate the relative distribution between the cells. The small standard error indicates that the differences in flux rates between different neighbouring cells are highly reproducible and that these differences are independent of the amount of DRONPA-s activated in each single experiment.

A big advantage of DRONPA-s is the fact that it is a non-invasive tool, given that a precise activation of DRONPA-s in individual cells by low amounts of energy, and thus less harmful light, is possible using a a two-photon laser. The ability to activate single cells is particularly beneficial for studying complex tissues such as the root tip, where individual cells differ in size, shape or type. By adjusting the activation time, the fluorescence intensity can be well regulated to avoid saturation and allow quantification of the fluorescence intensity. Another advantage of DRONPA-s compared with other activatable fluorescent proteins is that DRONPA is very bright, has a low background and can also be used in deeper tissue layers. Furthermore it can be switched on and off repeatedly, which means that there is no need to change the sample after each activation step. We didn't observe any difference in the flux behaviour after repeated on and off switches, which indicates that the root is not severely stressed by these treatments. In addition, the tissue was stained by PI, which is also used as an indicator of cell damage: when the plasma membrane is injured the stain enters the cell and stains the nucleus. We never observed induction of PI staining in a nucleus by activation or deactivation of DRONPA-s. We also showed that the system is appropriate for monitoring inducible changes in the SEL. In summary we conclude that the DRONPA-s based system is useful for comparative analyses of symplasmic connectivity between plant cells in general.

EXPERIMENTAL PROCEDURES

Plant transformation and growth conditions

Arabidopsis thaliana (Col0) was stably transformed with pCambia-CaMV-DRONPA-s DNA (Lummer *et al.*, 2011) according to the floral dip method (Clough and Bent, 1998) using the bacterial -strain C58C1 (Deblaere *et al.*, 1985) and grown in growth chambers (16-h light\8-h dark, 22°C) on soil or on plates containing MS medium [0.49% MS including vitamins/2-(*N*-morpholine)-ethanesulphonic acid (MES); Duchefa, https://www.duchefa-biochemie.com/], 2% saccharose, pH 5.7, 0.8% Phytagar (Duchefa).

Microscopy

Three-day-old seedlings grown on MS plates were transferred to 0.1% PI solution for cell wall staining as described previously (Stadler *et al.*, 2005a). Root tips were analysed using a Leica TCS SP5 II confocal microscope (Leica Microsystems, https://www.leica-microsystems.com/). Propidium iodide was excited at 488 nm and detected at 626-724 nm. Fluorescence intensities were quantified using Leica LAS AF software. DRONPA-s movement was analysed as follows:

(i) DRONPA-s deactivation: tissues were irradiated with 488-nm laser light for 30 sec and 70% of total laser intensity (argon laser, ~20 mW, Leica Microsystems), which corresponds to a six-fold higher photon density than what is generally used for a conventional single scan.
(ii) DRONPA-s activation: ROIs were set in the centre of the target cell without contacting the cell wall to avoid fluorescence activation in adjacent cells. The ROIs were exposed to 800-nm light for 20–40 sec using two-photon equipment (Mai Tai HP two-photon laser, Newport Spectra-Physics, https://www.newport.com/).
(iii) DRONPA-s detection: tissues were exposed to 488-nm laser light (argon laser). DRONPA-s emission was detected 10 min after single-cell-activation at 500-541 nm. The pinhole was kept at Airy 1. Saturation was avoided during all experiments. Successful single-cell-activation was controlled optically during all experiments.

Stress conditions

For flagellin treatment, 3-day-old seedlings were transferred to plates containing MS + 2 μM flg22 for 24 h. For SA treatment, seedlings were grown on plates containing MS + 100 μM SA for 72 h. For cold treatment, plates containing 3-day-old seedlings were transferred into a cooling chamber (4–6°C) for 2 h. After that, roots were stained with PI, cut off with a razor blade and transferred into a 22°C water droplet for 5 min prior to the measurement to prevent an inhibition of diffusion caused by low temperature. For all stress treatments, five to ten roots were analysed per experiment and independent mock treatments were performed as controls.

ACKNOWLEDGEMENTS

We thank Angelika Wolf for excellent technical assistance. We also thank Martina Lummer for kindly providing *pCambia-CaMV DRONPA-s* DNA.

CONFLICT OF INTEREST

The authors confirm no conflicts of interest.

SUPPORTING INFORMATION

Additional Supporting Information may be found in the online version of this article.
Figure S1. DRONPA-s flow from columella initials.
Figure S2. DRONPA-s flow from a root hair cell and a differentiated epidermal cell.
Data S1. ClickPoints guide.
Data S2. Flow model.

REFERENCES

Amsbury, S., Kirk, P. and Benitez-Alfonso, Y. (2018) Emerging models on the regulation of intercellular transport by plasmodesmata-associated callose. *J. Exp. Bot.* **69**, 105–115.
Ando, R., Mizuno, H. and Miyawaki, A. (2004) Regulated fast nucleocytoplasmic shuttling observed by reversible protein highlighting. *Science*, **306**, 1370–1373.
Bell, K. and Oparka, K. (2011) Imaging plasmodesmata. *Protoplasma*, **248**, 9–25.
Benitez-Alfonso, Y., Faulkner, C., Ritzenthaler, C. and Maule, A.J. (2010) Plasmodesmata: gateways to local and systemic virus infection. *Mol Plant-Microbe Interact*, **23**, 1403–1412.
Bilska, A. and Sowinski, P. (2010) Closure of plasmodesmata in maize (Zea mays) at low temperature: A new mechanism for inhibition of photosynthesis. *Ann. Bot.* **106**, 675–686.
Bishopp, A., Lehesranta, S., Vatén, A., Help, H., El-Showk, S., Scheres, B., Helariutta, K., Mähönen, A.P., Sakakibara, H. and Helariutta, Y. (2011) Phloem-transported cytokinin regulates polar auxin transport and maintains vascular pattern in the root meristem. *Curr. Biol.* **21**, 927–932.
Botha, CEJ, Hartley, BJ and Cross, RHM. (1993) The ultrastructure and computer-enhanced digital image analysis of plasmodesmata at the kranz mesophyll-bundle sheath interface of Themeda triandra var. imberbis (Retz) A. Camus in conventionally-fixed leaf blades. *Ann. Bot.* **72**, 255–261.
Brunkard, J.O. and Zambryski, P.C. (2017) Plasmodesmata enable multicellularity: new insights into their evolution, biogenesis, and functions in development and immunity. *Curr. Opin. Plant Biol.* **35**, 76–83.
Burch-Smith, T.M. and Zambryski, P.C. (2010) Loss of INCREASED SIZE EXCLUSION LIMIT (ISE)1 or ISE2 increases the formation of secondary plasmodesmata. *Curr. Biol.* **20**, 989–993.
Cantrill, L.C., Overall, R.L. and Goodwin, P.B. (2001) Changes in symplastic permeability during adventitious shoot regeneration in tobacco thin cell layers. *Planta*, **214**, 206–214.
Cantrill, L.C., Overall, R.L. and Goodwin, P.B. (2005) Changes in macromolecular movement accompany organogenesis in thin cell layers of Torenia fournieri. *Planta*, **222**, 933–946.
Carlsbecker, A., Lee, J.-Y., Roberts, C.J. *et al.* (2010) Cell signalling by microRNA165/6 directs gene dose-dependent root cell fate. *Nature*, **465**, 316–321.
Cheval, C. and Faulkner, C. (2018) Plasmodesmal regulation during plant-pathogen interactions. *New Phytol.* **217**, 62–67.
Christensen, N.M., Faulkner, C. and Oparka, K. (2009) Evidence for unidirectional flow through plasmodesmata. *Plant Physiol.* **150**, 96–104.
Clough, S.J. and Bent, A.F. (1998) Floral dip: a simplified method for Agrobacterium-mediated transformation of Arabidopsis thaliana. *Plant J.* **16**, 735–743.
Crawford, K.M. and Zambryski, P.C. (2000) Subcellular localization determines the availability of non-targeted proteins to plasmodesmatal transport. *Curr. Biol.* **10**, 1032–1040.
Cui, W. and Lee, J.-Y. (2016) Arabidopsis callose synthases CalS1/8 regulate plasmodesmal permeability during stress. *Nat Plants*, **2**, 16034.
Cui, H., Levesque, MP., Vernoux, T., Jung, JW., Paquette, AJ., Gallagher, KL., Wang, JY., Blilou, I., Scheres, B. and Benfey, PN. (2007) An evolutionarily conserved mechanism delimiting SHR movement defines a single layer of endodermis in plants. *Science*, **316**, 421–425.
Cui, H., Hao, Y., Kovtun, M., Stolc, V., Deng, X.-W., Sakakibara, H. and Kojima, M. (2011) Genome-wide direct target analysis reveals a role for SHORT-ROOT in root vascular patterning through cytokinin homeostasis. *Plant Physiol.* **157**, 1221–1231.
Deblaere, R., Bytebier, B., De Greve, H., Deboeck, F., Schell, J., Van Montagu, M. and Leemans, J. (1985) Efficient octopine Ti plasmid-derived vectors for Agrobacterium-mediated gene transfer to plants. *Nucleic Acids Res.* **13**, 4777–4788.
Ding, B., Turgeon, R. and Parthasarathy, M.V. (1992) Substructure of freeze-substituted plasmodesmata. *Protoplasma*, **169**, 28–41.
Duckett, C.M., Oparka, K.J., Prior, D.A.M., Dolan, L. and Roberts, K. (1994) Dye-coupling in the root epidermis of Arabidopsis is progressively reduced during development. *Development*, **120**, 3247–3255.
Faulkner, C., Petutschnig, E., Benitez-Alfonso, Y., Beck, M., Robatzek, S., Lipka, V. and Maule, A.J. (2013) LYM2-dependent chitin perception limits molecular flux via plasmodesmata. *Proc Natl Acad Sci U S A*, **110**, 9166–9170.
Fisher, D.B. and Cash-Clark, C.E. (2000) Sieve tube unloading and post-phloem transport of fluorescent tracers and proteins injected into sieve tubes via severed aphid stylets. *Plant Physiol.* **123**, 125–138.
Fitzgibbon, J., Bell, K., King, E. and Oparka, K. (2010) Super-resolution imaging of plasmodesmata using three-dimensional structured illumination microscopy. *Plant Physiol.* **153**, 1453–1463.
Fitzgibbon, J., Beck, M., Zhou, J., Faulkner, C., Robatzek, S. and Oparka, K. (2013) A developmental framework for complex plasmodesmata formation revealed by large-scale imaging of the Arabidopsis leaf epidermis. *Plant Cell*, **25**, 57–70.
Gallagher, K.L., Paquette, A.J., Nakajima, K. and Benfey, P.N. (2004) Mechanisms regulating SHORT-ROOT intercellular movement. *Curr. Biol.* **14**, 1847–1851.

Gallagher, K.L., Sozzani, R. and Lee, C.-M. (2014) Intercellular protein movement: deciphering the language of development. *Annu. Rev. Cell Dev. Biol.* **30**, 207–233.

Gerum, R.C., Richter, S., Fabry, B. and Zitterbart, D.P. (2016) ClickPoints: An expandable toolbox for scientific image annotation and analysis. *Methods Ecol. Evol.* **8**, 750–756.

Gisel, A., Barella, S., Hempel, F.D. and Zambryski, P.C. (1999) Temporal and spatial regulation of symplastic trafficking during development in Arabidopsis thaliana apices. *Development*, **126**, 1879–1889.

Gómez-Gómez, L. and Boller, T. (2000) FLS2: an LRR receptor-like kinase involved in the perception of the bacterial elicitor flagellin in arabidopsis. *Mol. Cell*, **5**, 1003–1011.

Grabski, S., De Feijter, A.W. and Schindler, M. (1993) Endoplasmic reticulum forms a dynamic continuum for lipid diffusion between contiguous soybean root cells. *Plant Cell*, **5**, 25–38.

Gunning, B.E.S. (1978) Age-related and origin-related control of the numbers of plasmodesmata in cell walls of developing Azolla roots. *Planta*, **143**, 181–190.

Haupt, S., Duncan, G.H., Holzberg, S. and Oparka, K.J. (2001) Evidence for symplastic phloem unloading in sink leaves of barley. *Plant Physiol.* **125**, 209–218.

Helariutta, Y., Fukaki, H., Wysocka-Diller, J., Nakajima, K., Jung, J., Sena, G., Hauser, M.T. and Benfey, P.N. (2000) The SHORT-ROOT gene controls radial patterning of the Arabidopsis root through radial signaling. *Cell*, **101**, 555–567.

Holdaway-Clarke, T.L., Walker, N.A. and Overall, R.L. (1996) Measurement of the electrical resistance of plasmodesmata and membranes of corn suspension-culture cells. *Planta*, **199**, 537–544.

Holdaway-Clarke, T.L., Walker, N.A., Hepler, P.K. and Overall, R.L. (2000) Physiological elevations in cytoplasmic free calcium by cold or ion injection result in transient closure of higher plant plasmodesmata. *Planta*, **210**, 329–335.

Imlau, A., Truernit, E. and Sauer, N. (1999) Cell-to-Cell and long-distance trafficking of the green fluorescent protein in the phloem and symplastic unloading of the protein into sink tissues. *Plant Cell*, **11**, 309–322.

Jackson, D. (2015) Plasmodesmata spread their influence. *F1000 Prime Reports* **7**, 1–7.

Jones, D.L., Blancaflor, E.B., Kochian, L.V. and Gilroy, S. (2006) Spatial coordination of aluminium uptake, production of reactive oxygen species, callose production and wall rigidification in maize roots. *Plant, Cell Environ.* **29**, 1309–1318.

Lee, J.-Y., Wang, X., Cui, W. *et al.* (2011) A plasmodesmata-localized protein mediates crosstalk between cell-to-cell communication and innate immunity in arabidopsis. *Plant Cell*, **23**, 3353–3373.

Levesque, M.P., Vernoux, T., Busch, W. *et al.* (2006) Whole-Genome analysis of the SHORT-ROOT developmental pathway in arabidopsis. *PLoS Biol.* **4**, e249.

Li, S., He, Y., Zhao, J., Zhang, L. and Sun, M.X. (2013) Polar protein transport between apical and basal cells during tobacco early embryogenesis. *Plant. Cell. Rep.* **32**, 285–291.

Liarzi, O. and Epel, B.L. (2005) Development of a quantitative tool for measuring changes in the coefficient of conductivity of plasmodesmata induced by developmental, biotic, and abiotic signals. *Protoplasma*, **225**, 67–76.

Liesche, J. and Schulz, A. (2012) In vivo quantification of cell coupling in plants with different phloem-loading strategies. *Plant Physiol.* **159**, 355–365.

Liesche, J. and Schulz, A. (2013) Modeling the parameters for plasmodesmal sugar filtering in active symplasmic phloem loaders. *Front Plant Sci*, **4**, 207.

Lim, G.-H., Kachroo, A. and Kachroo, P. (2016) Role of plasmodesmata and plasmodesmata localizing proteins in systemic immunity. *Plant Signal Behav*, **11**, e1219829.

Lu, K-J., De Rybel, B., van Mourik, H. and Weijers, D. (2018) Regulation of intercellular TARGET OF MONOPTEROS 7 protein transport in the Arabidopsis root. *Development* **145**, dev152892.

Lucas, W.J. and Lee, J.-Y. (2004) Plasmodesmata as a supracellular control network in plants. *Nat. Rev. Mol. Cell Biol.* **5**, 712–726.

Lucas, W.J., Yoo, B.-C. and Kragler, F. (2001) RNA as a long-distance information macromolecule in plants. *Nat. Rev. Mol. Cell Biol.* **2**, 849–857.

Lummer, M., Humpert, F., Steuwe, C., Caesar, K., Schüttpelz, M., Sauer, M. and Staiger, D. (2011) Reversible photoswitchable DRONPA-s monitors nucleocytoplasmic transport of an RNA-binding protein in transgenic plants. *Traffic*, **12**, 693–702.

Martens, H.J., Hansen, M. and Schulz, A. (2004) Caged probes: a novel tool in studying symplasmic transport in plant tissues. *Protoplasma*, **223**, 63–66.

Martens, H.J., Roberts, A.G., Oparka, K.J. and Schulz, A. (2006) Quantification of plasmodesmatal endoplasmic reticulum coupling between sieve elements and companion cells using fluorescence redistribution after photobleaching. *Plant Physiol.* **142**, 471–480.

McCaskill, A. and Turgeon, R. (2007) Phloem loading in Verbascum phoeniceum L. depends on the synthesis of raffinose-family oligosaccharides. *Proc Natl Acad Sci U S A*, **104**, 19619–19624.

Miyashima, S., Koi, S., Hashimoto, T. and Nakajima, K. (2011) Non-cell-autonomous microRNA165 acts in a dose-dependent manner to regulate multiple differentiation status in the Arabidopsis root. *Development*, **138**, 2303–2313.

Nakajima, K., Sena, G., Nawy, T. and Benfey, P.N. (2001) Intercellular movement of the putative transcription factor SHR in root patterning. *Nature*, **413**, 307–311.

Nicolas, W., Grison, M.S., Trepout, S., Gaston, A., Fouché, M., Cordelières, F.P., Oparka, K.J., Tilsner, J., Brocard, L. and Bayer, E.M. (2017) Architecture and permeability of post-cytokinesis plasmodesmata lacking cytoplasmic sleeves. *Nat Plants*, **69**, 91–103.

Ogasawara, H., Kaimi, R., Colasanti, J. and Kozaki, A. (2011) Activity of transcription factor JACKDAW is essential for SHR/SCR-dependent activation of SCARECROW and MAGPIE and is modulated by reciprocal interactions with MAGPIE, SCARECROW and SHORT ROOT. *Plant Mol. Biol.* **77**, 489.

Oide, S., Bejai, S., Staal, J., Guan, N., Kaliff, M. and Dixelius, C. (2013) A novel role of PR2 in abscisic acid (ABA) mediated, pathogen-induced callose deposition in Arabidopsis thaliana. *New Phytol.* **200**, 1187–1199.

Oparka, K., Prior, D.A.M. and Wright, K. (1995) Symplastic communication between primary and developing lateral roots of Arabidopsis thaliana. *J. Exp. Bot.* **45**, 187–197.

Oparka, K.J., Roberts, A.G., Boevink, P., Cruz, S.S., Roberts, I., Pradel, K.S., Imlau, A., Kotlizky, G., Sauer, N. and Epel, B. (1999) Simple, but Not branched, plasmodesmata allow the nonspecific trafficking of proteins in developing tobacco leaves. *Cell*, **97**, 743–754.

Otero, S., Helariutta, Y. and Benitez-Alfonso, Y. (2016) Symplastic communication in organ formation and tissue patterning. *Curr. Opin. Plant Biol.* **29**, 21–28.

Overall, R.L. and Blackman, L.M. (1996) A model of the macromolekular structure of plasmodesmata. *Trends Plant Sci.* **1**, 307–311.

Palevitz, B.A. and Hepler, P.K. (1985) Changes in dye coupling of stomatal cells of Allium and Commelina demonstrated by microinjection of Lucifer yellow. *Planta*, **164**, 473–479.

Pi, L., Aichinger, E., van der Graaff, E., Llavata-Peris, C.I., Weijers, D., Hennig, L., Groot, E. and Laux, T. (2015) Organizer-derived WOX5 signal maintains root columella stem cells through chromatin-mediated repression of CDF4 expression. *Dev. Cell*, **33**, 576–588.

Rim, Y., Jung, J.-H., Chu, H., Kyong Cho, W., Kim, S.-W., Hong, J.C., Jackson, D., Datla, R. and Kim, Y.-J. (2009) A non-cell-autonomous mechanism for control of plant architecture and epidermal differentiation involves intercellular trafficking of BREVIPEDICELLUS protein. *Funct. Plant Biol.* **36**, 280–289.

Rinne, P.L. and van der Schoot, C. (1998) Symplasmic fields in the tunica of the shoot apical meristem coordinate morphogenetic events. *Development*, **125**, 1477–1485.

Robards, A.W. (1971) The ultrastructure of plasmodesmata. *Protoplasma*, **72**, 315–323.

Roberts, A.G. and Oparka, K.J. (2003) Plasmodesmata and the control of symplastic transport. *Plant, Cell Environ.* **26**, 103–124.

Roberts, A.G., Cruz, S.S., Roberts, I.M., Prior, D.A.M., Turgeon, R. and Oparka, K.J. (1997) Phloem unloading in sink leaves of Nicotiana benthamiana: comparison of a fluorescent solute with a fluorescent virus. *Plant Cell*, **9**, 1381–1396.

Roberts, I.M., Boevink, P., Roberts, A.G., Sauer, N., Reichel, C. and Oparka, K.J. (2001) Dynamic changes in the frequency and architecture of plasmodesmata during the sink-source transition in tobacco leaves. *Protoplasma*, **218**, 31–44.

Roslan, H.A., Salter, M.G., Wood, C.D. *et al.* (2001) Characterization of the ethanol-inducible alc gene-expression system in Arabidopsis thaliana. *Plant J.* **28**, 225–235.

Ross-Elliott, T.J., Jensen, K.H., Haaning, K.S. *et al.* (2017) Phloem unloading in Arabidopsis roots is convective and regulated by the phloempole pericycle. *Elife* **6**, e24125. https://doi.org/10.7554/eLife.24125.001.

Rutschow, H.L., Baskin, T.I. and Kramer, E.M. (2011) Regulation of solute flux through plasmodesmata in the root meristem. *Plant Physiol.* **155**, 1817–1826.

Sager, R. and Lee, J.Y. (2014) Plasmodesmata in integrated cell signalling: Insights from development and environmental signals and stresses. *J. Exp. Bot.* **65**, 6337–6358.

Schulz, A. (1999) Physiological control of plasmodesmal gating. In van Bel, AJE, Van Kesteren, WJP, eds, *Plasmodesmata Struct. Funct. Role Cell Commun*. Berlin, Heidelberg: Springer Berlin Heidelberg, pp 173–204.

Sena, G., Jung, J.W. and Benfey, P.N. (2004) A broad competence to respond to SHORT ROOT revealed by tissue-specific ectopic expression. *Development*, **131**, 2817–2826.

Sivaguru, M., Fujiwara, T., Šamaj, J., Baluška, F., Yang, Z., Osawa, H., Maeda, T., Mori, T., Volkmann, D. and Matsumoto, H. (2000) Aluminum-induced 1→3-β-d-glucan inhibits cell-to-cell trafficking of molecules through plasmodesmata. a new mechanism of aluminum toxicity in plants. *Plant Physiol.* **124**, 991–1006.

Stadler, R., Lauterbach, C. and Sauer, N. (2005a) Cell-to-cell movement of green fluorescent protein reveals post-phloem transport in the outer integument and identifies symplastic domains in arabidopsis seeds and embryos. *Plant Physiol.* **139**, 701–712.

Stadler, R., Wright, K.M., Lauterbach, C., Amon, G., Gahrtz, M., Feuerstein, A., Oparka, K.J. and Sauer, N. (2005b) Expression of GFP-fusions in Arabidopsis companion cells reveals non-specific protein trafficking into sieve elements and identifies a novel post-phloem domain in roots. *Plant J.* **41**, 319–331.

Stahl, Y. and Faulkner, C. (2016) Receptor complex mediated regulation of symplastic traffic. *Trends Plant Sci.* **21**, 450–459.

Stonebloom, S., Brunkard, J.O., Cheung, A.C., Jiang, K., Feldman, L. and Zambryski, P. (2012) Redox states of plastids and mitochondria differentially regulate intercellular transport via plasmodesmata. *Plant Physiol.* **158**, 190–199.

Terry, B.R. and Robards, A.W. (1987) Hydrodynamic radius alone governs the mobility of molecules through plasmodesmata. *Planta*, **171**, 145–157.

Thomas, C.L., Bayer, E.M., Ritzenthaler, C., Fernandez-Calvino, L. and Maule, A.J. (2008) Specific targeting of a plasmodesmal protein affecting cell-to-cell communication. *PLoS Biol.* **6**, 0180–0190.

Tucker, E.B. (1982) Translocation in the staminal hairs of Setcreasea purpurea. *Protoplasma*, **113**, 193–201.

Turgeon, R. and Gowan, E. (1990) Phloem loading in coleus blumei in the absence of carrier-mediated uptake of export sugar from the apoplast. *Plant Physiol.* **94**, 1244–1249.

Ueki, S. and Citovsky, V. (2005) Identification of an interactor of cadmium ion-induced glycine-rich protein involved in regulation of callose levels in plant vasculature. *Proc Natl Acad Sci U S A*, **102**, 12089–12094.

Vatén, A., Dettmer, J., Wu, S. *et al.* (2011) Callose biosynthesis regulates symplastic trafficking during root development. *Dev. Cell*, **21**, 1144–1155.

Waigmann, E., Turner, A., Peart, J., Roberts, K. and Zambryski, P. (1997) Ultrastructural analysis of leaf trichome plasmodesmata reveals major differences from mesophyll plasmodesmata. *Planta*. **203**, 75–84.

Wang, X., Sager, R., Cui, W., Zhang, C., Lu, H. and Lee, J.-Y. (2013) Salicylic acid regulates plasmodesmata closure during innate immune responses in arabidopsis. *Plant Cell*, **25**, 2315–2329.

Welch, D., Hassan, H., Blilou, I., Immink, R., Heidstra, R. and Scheres, B. (2007) Arabidopsis JACKDAW and MAGPIE zinc finger proteins delimit asymmetric cell division and stabilize tissue boundaries by restricting SHORT-ROOT action. *Genes Dev.* **21**, 2196–2204.

Werner, D., Gerlitz, N. and Stadler, R. (2011) A dual switch in phloem unloading during ovule development in Arabidopsis. *Protoplasma*, **248**, 225–235.

Wille, A.C. and Lucas, W.J. (1984) Ultrastructural and histochemical studies on guard cells. *Planta*, **160**, 129–142.

Willmer, C.M. and Sexton, R. (1979) Stomata and plasmodesmata. *Protoplasma*, **100**, 113–124.

Wolf, S., Lucas, W.J., Deom, C.M. and Beachy, R.N. (1989) Movement protein of tobacco mosaic virus modifies plasmodesmatal size exclusion limit. *Science*, **246**, 377–379.

Wright, K.M. and Oparka, K.J. (1996) The fluorescent probe HPTS as a phloem-mobile, symplastic tracer: An evaluation using confocal laser scanning microscopy. *J. Exp. Bot.* **47**, 439–445.

Wu, S., Koizumi, K., Macrae-Crerar, A. and Gallagher, K.L. (2011) Assessing the utility of photoswitchable fluorescent proteins for tracking intercellular protein movement in the Arabidopsis root. *PloS ONE*, **6**, e27536.

Zhu, T., Lucas, W.J. and Rost, T.L. (1998a) Directional cell-to-cell communication in the Arabidopsis root apical meristem I. An ultrastructural and functional analysis. *Protoplasma*, **203**, 35–47.

Zhu, T., Quinn, R.L.O., Lucas, W.J. and Rost, T.L. (1998b) Directional cell-to-cell communication in Arabidopsis root apical meristem. II. Dynamics of plasmodesmatal formation. *Protoplasma*, **204**, 84–93.